ISSN 1070-3632, Russian Journal of General Chemistry, 2018, Vol. 88, No. 1, pp. 114–119. © Pleiades Publishing, Ltd., 2018.
Original Russian Text © A.G. Belous, O.I. V'yunov, S.D. Kobylyanskaya, A.A. Ishchenko, A.V. Kulinich, 2018, published in Zhurnal Obshchei Khimii, 2018, Vol. 88, No. 1, pp. 120–125.

Influence of Synthesis Conditions on the Morphology and Spectral-Luminescent Properties of Films of Organic-Inorganic Perovskite $CH_3NH_3PbI_{2.98}Cl_{0.02}$

A. G. Belous[a], O. I. V'yunov[a]*, S. D. Kobylyanskaya[a], A. A. Ishchenko[b], and A. V. Kulinich[b]

[a] *Vernadskii Institute of General and Inorganic Chemistry, National Academy of Sciences of Ukraine, pr. Akademika Palladina 32/34, Kiev, 03680 Ukraine*
**e-mail: vyunov@ionc.kiev.ua*

[b] *Institute of Organic Chemistry, National Academy of Sciences of Ukraine, Kiev, Ukraine*

Received July 6, 2017

Abstract—The influence of the synthesis conditions (rotation speed used for spin-coating deposition of the film, film drying temperature, and the ratio of the PbI_2 and CH_3NH_3I reactants in solutions) on the microstructure, phase composition, and spectral-luminescent properties of films of organic-inorganic perovskite $CH_3NH_3PbI_{3-x}Cl_x$ (x = 0, 0.02) was elucidated.

Keywords: organic-inorganic perovskite, X-ray phase analysis, microstructure, absorption and luminescence spectra

DOI: 10.1134/S1070363218010188

Inorganic crystalline materials of the ABO_3 perovskite structure find extensive use in many engineering applications, e.g., as condenser materials [1, 2], materials with positive temperature coefficient [3, 4], lithium ion-conducting materials [5, 6], materials displaying large magnetoresistance effect [7, 8], high-quality factor microwave dielectrics [9, 10], piezoelectric materials [11, 12], etc. First demonstration of the suitability of organic-inorganic halides ABX_3 (isomorphic to the $CaTiO_3$ perovskite structure, where B = Pb or Sn, X = Cl, Br, I; A = $CH_3NH_3^+$) for converting solar energy with ~10% power conversion efficiency (PCE) [13, 14] set off a research boom in this field. Within 3–4 years, 20% PCE was achieved [15], with theoretical limit being just above 30% [16]. Comparative simplicity of production [15] makes these organic-inorganic halides highly promising for development of low-cost high-efficiency solar cells.

One of the factors determining the efficiency of organic-inorganic perovskites as photovoltaic converters is the internal morphology of the material. Different photovoltaic effects are observed for different faces of perovskite microcrystals, with some faces exhibiting PCE of 30% approaching the theoretical maximum [17, 18]. Consequently, by varying the size and arrangement of perovskite microcrystals, as well as the photoactive layer thickness, it is possible to optimize its efficiency. Therefore, elucidation of the influence of the synthesis conditions on the morphology of perovskites is a topical research task.

In solutions of precursors used for synthesis of organic-inorganic perovskites, the formation of various complexes (PbI_3^-, PbI_4^{2-}) differently affecting the microstructure of the final film is observed [19]. In particular, a change in the stoichiometric ratio of CH_3NH_3I : PbI_2 in the precursor solutions significantly alters the film microstructure [20]. These findings agree with the stability of hybrid halide perovskites with respect to the phase separation reaction ($CH_3NH_3PbI_3 \rightarrow CH_3NH_3I + PbI_2$) from *ab initio* calculations [21]. For $CH_3NH_3PbI_3$ this reaction is thermodynamically favorable, i.e., it may occur spontaneously even without any moisture, oxygen, or illumination in the environment. This degradation reaction, however, is kinetically limited, i.e., $CH_3NH_3PbI_3$ can be stable for a certain period of time. Suppression of the $CH_3NH_3PbI_3$ degradation (essential for practical purposes) requires increasing the kinetic barrier of the phase separation. Thermodynamic calculations [21] revealed higher stability of the structure of partially

substituted halide perovskites (e.g., of those with I substituted by Cl) compared to the original $CH_3NH_3PbI_3$ and also of the orthorhombic compared to tetragonal structures.

The synthesis of organic-inorganic perovskites on glass substrates in the absence of a mesoporous layer is relatively poorly described in the literature. Also, there is no information on the influence of the CH_3NH_3I : PbI_2 ratio in the precursor solutions on the microstructure, phase composition, and absorption and luminescence spectra of the resulting films.

Here, we synthesized films of organic-inorganic perovskite $CH_3NH_3PbI_{3-x}Cl_x$ on a glass substrate in the absence of a mesoporous layer and examined how the synthesis conditions (rotation speed of the substrate during spin-coating deposition of the film, film drying temperature, and ratio of the reactants PbI_2 : CH_3NH_3I in the precursor solutions) affected the microstructure, morphology, phase composition, and spectral-luminescent properties of the films.

In the first stage we investigated conditions for the synthesis of organic-inorganic perovskites at a 1 : 1 ratio of the reactants PbI_2 and CH_3NH_3I. The synthesis was carried out in an air atmosphere (55–65% humidity). As shown by X-ray phase analysis, the resulting film was composed of two phases, $CH_3NH_3PbI_3$ and PbI_2 (peaks at 2θ = 13° and 26°). The $CH_3NH_3PbI_3$ sample synthesized in a dry box contained, along with the perovskite phase, 15–20% of unknown phase X1 (2θ = 9.5°, 22.6°). The latter presumably resulted from intercalation of CH_3NH_3I and DMF in PbI_2 (similarly to the CH_3NH_3I–PbI_2–DMSO intermediate phase [22]). The X-ray diffraction patterns obtained at room temperature are indexed in tetragonal crystal system I4/mcm, in agreement with published data [23, 24].

In the second stage, 2 mol % of CH_3NH_3Cl was introduced to enhance the stability of the perovskite structure (see [21]). Partial substitution of the anion led to the production of a single-phase solid solution $CH_3NH_3PbI_{2.98}Cl_{0.02}$ (Fig. 1, curve *1*), as contrasted with $CH_3NH_3PbI_3$. Further, we examined the $CH_3NH_3PbI_{2.98}Cl_{0.02}$ perovskite.

Heat treatment at 80°C yielded a single-phase perovskite $CH_3NH_3PbI_{2.98}Cl_{0.02}$ film (Fig. 1, curve *1*). At 90°C trace amounts of the unknown phase X1 appeared. The X-ray diffraction peaks from this phase disappeared as the temperature increased to 95°C. At 100°C, peaks of PbI_2 appeared and grew in intensity

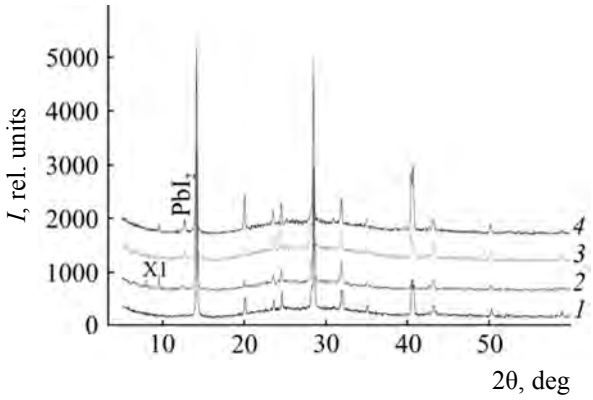

Fig. 1. X-ray diffraction patterns of the $CH_3NH_3PbI_{2.98}Cl_{0.02}$ films heat-treated in air at (*1*) 80, (*2*) 90, (*3*) 100, and (*4*) 110°C.

with further increase in temperature (Fig. 1, curves *3* and *4*), thereby indicating thermal degradation of the perovskite.

Interferometric analysis of the $CH_3NH_3PbI_{2.98}Cl_{0.02}$ film deposited on a glass substrate by the spin-coating procedure revealed the thickness of 500 nm for the rotation speed of 20 rpm and that of 400 nm for 40 rpm. Irrespective of the rotation speed, the film was of nonuniform thickness. Examination of the microstructure of the resultant samples showed that the films crystallized into needle-like structures arranged along the substrate plane (Figs. 2a and 2b). In the film obtained at rotation speed of 40 rpm these particles were arranged predominantly within one layer, and in the case of 20 rpm the needles partially overlap, making the film thicker and of more nonuniform thickness.

The shape of the particles is determined by the substrate surface preparation procedure. Nuclei resulted from film deposition on surface-nonactivated glass substrates are characterized by a larger spread in size, since nucleation proceeds on substrate defects for the most part [25]. In our experiments we used such substrate, so the resulting perovskite particles were shape-anisotropic, disorderly arranged over the surface.

Films obtained at different rotation speeds differ in the phase composition as well. The X-ray diffraction patterns of the films deposited at 20 rpm speed contained, along with peaks from the perovskite phase, peaks from unknown phase X1, and the spin-coating process ran at 40 rpm speed gave a single-phase film. Therefore, the solvent evaporation rate affects the phase composition of the films, in agreement with

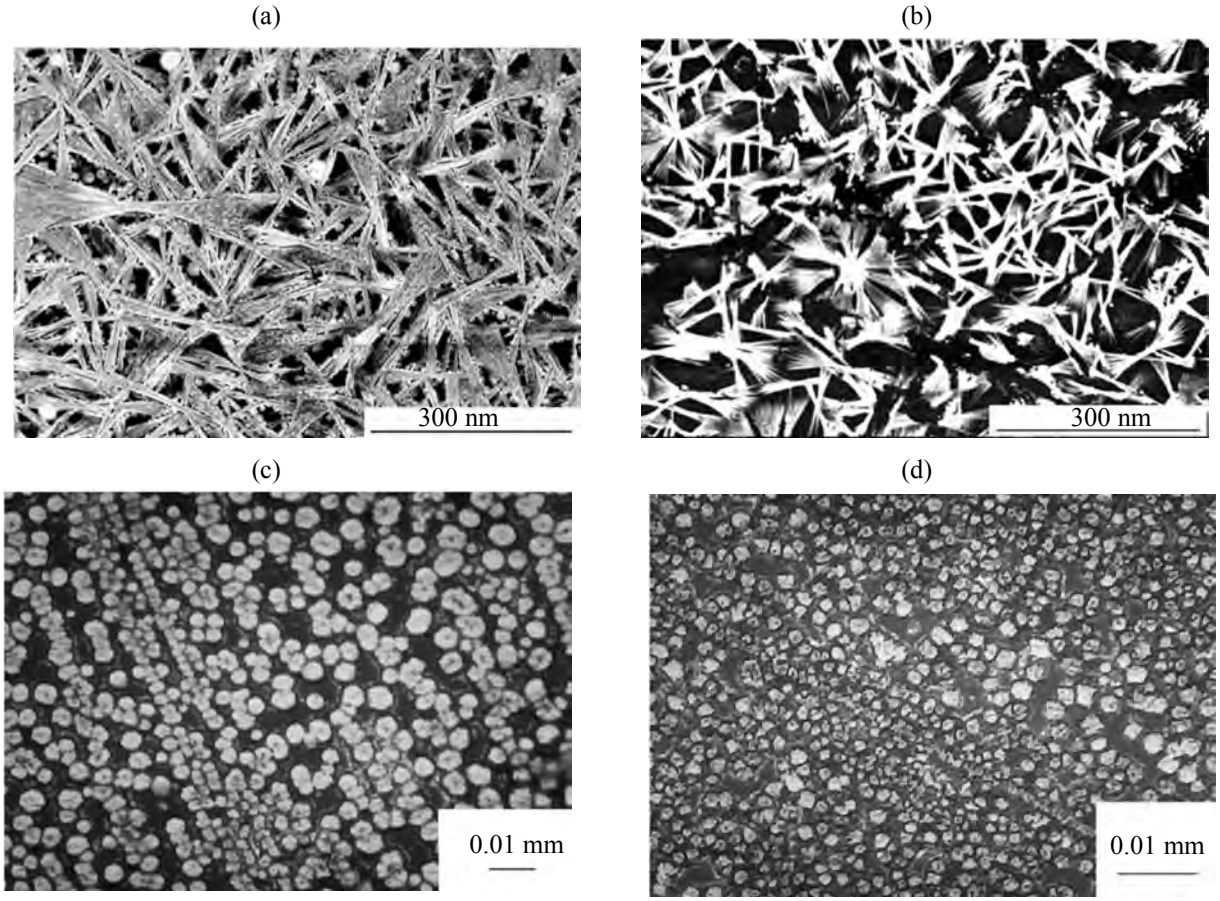

Fig. 2. Microstructure of the $CH_3NH_3PbI_{2.98}Cl_{0.02}$ films obtained at the PbI_2 : CH_3NH_3I ratio of (a, b) 1 : 1 by spin-coating at the rotation speed of (a) 20 and (b) 40 rpm and of (c) 1 : 2 and (d) 1 : 3 at the rotation speed of 40 rpm.

published data, so the formation of single-phase films requires that the crystallization and solvent evaporation processes proceed at different times [26]. An increase in the rotation speed during film deposition causes the initial rate of the solvent evaporation to increase, while the crystallization rates in both versions are close.

In the third stage, we synthesized organic-inorganic perovskites $CH_3NH_3PbI_{2.98}Cl_{0.02}$ at different ratios of the reactants PbI_2 and CH_3NH_3I (1 : 1, 1 : 2, 1 : 3), with methylammonium iodide partially replaced by 2, 1, and 0.67 mol % of CH_3NH_3Cl. Synthesis at a 1 : 1 ratio gave a single-phase sample upon heat treatment at 80°C, and upon treatment at 150°C the sample contained a PbI_2 phase because of degradation of the original perovskite (Fig. 3). The sample synthesized at a 1 : 3 reactant ratio and heat-treated at 80°C contained residues of additional phases, which were removed by heat treatment at 150°C (Fig. 4). The process run at a 1 : 2 ratio led to the formation of a single-phase sample over a broad temperature range (Fig. 3).

Figure 4 presents the elemental composition data obtained by the EDX method for the $CH_3NH_3PbI_{2.98}Cl_{0.02}$ films synthesized from solutions at different reactant ratios. It is seen that the intensity ratios of the Pb and I peaks are identical for the samples synthesized at different PbI_2 : CH_3NH_3I ratios. Consequently, the stoichiometric composition of the perovskite films is unaffected by CH_3NH_3I excess in the precursor solution. Excessive CH_3NH_3I apparently decomposed into volatile components ($CH_3NH_3I \rightarrow CH_3NH_2\uparrow + HI\uparrow$) and was removed during annealing.

The shape and size of the $CH_3NH_3PbI_{2.98}Cl_{0.02}$ film particles depend on the stoichiometric ratio of the reactants. The films synthesized at PbI_2 : CH_3NH_3I = 1 : 1 ratio consisted of needles arranged along the substrate plane (Figs. 2a and 2b). At a 1 : 2 ratio round particles were formed (Fig. 2c); on further increase in the methylammonium iodide amount (PbI_2 : CH_3NH_3I = 1 : 3) a change to faceted particles was observed (Fig. 2d). The films synthesized at different ratios of

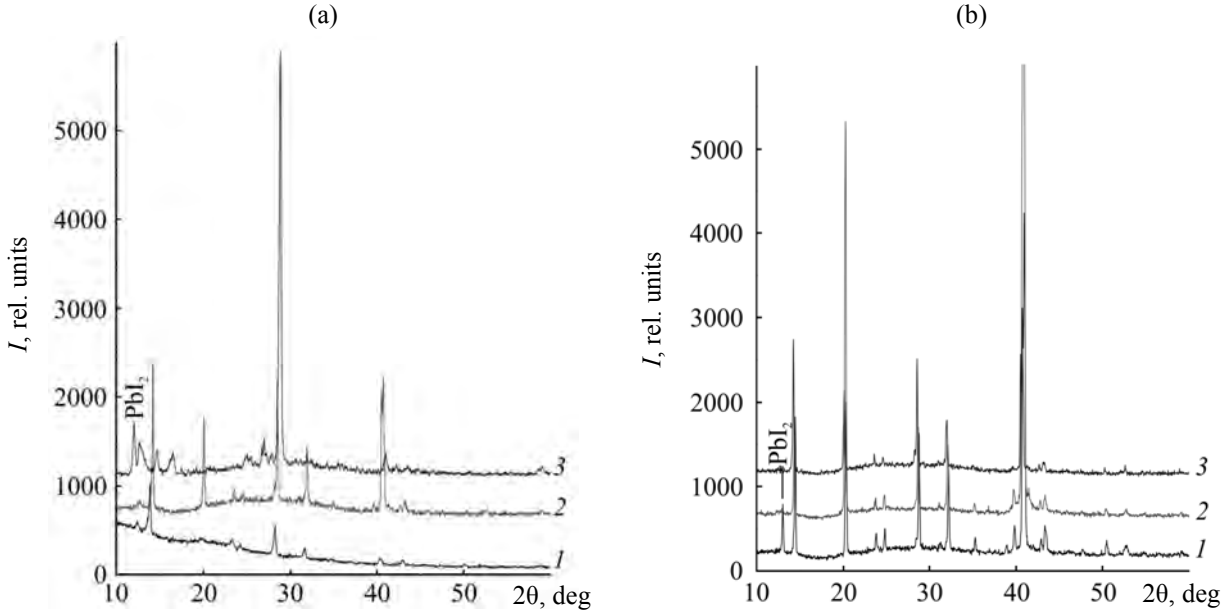

Fig. 3. X-ray diffraction patterns of the $CH_3NH_3PbI_{2.98}Cl_{0.02}$ films heat-treated at (a) 80 and (b) 150°C and prepared at the PbI_2 : CH_3NH_3I ratio of (*1*) 1 : 1, (*2*) 1 : 2, and (*3*) 1 : 3.

the reactants and heat-treated at 80°C were of the same thickness, 500 nm.

Comparison of the electron absorption spectra of the $CH_3NH_3PbI_{2.98}Cl_{0.02}$ films shows that, with the increasing CH_3NH_3I proportion in the precursor solution, the absorption becomes more selective. Specifically, the band at 350–400 nm grows in intensity, and in the visible spectral region the absorption declines (Fig. 5). For the precursor solution, the absorption occurs below 350 nm (Fig. 5a, curve *4*), with a band peaked near 327 nm indicating partial interaction of the mixture components in solution and formation of complexes [26]. The fluorescence intensity of the $CH_3NH_3PbI_{2.98}Cl_{0.02}$ films heat-treated at 80°C tends to increase with the reactant ratio changing in the (1 : 1)–(1 : 2)–(1 : 3) series (Fig. 5b). The same is true of the samples heat-treated at 150°C, although the fluorescence intensity is much lower in this case (cf. Fig. 5b, curves *3* and *4*). The band maxima (765 nm) in the luminescence spectra of the films synthesized at 1 : 2 and 1 : 3 ratio of components agree with the published data available for the perovskites of interest [28]. For the films synthesized at a 1 : 1 ratio the fluorescence band exhibits a red shift (Fig. 5b), due apparently to a greater optical density at the long-wave edge of the absorption band of this film (Fig. 5a). The stoichiometric compositions of the resulting films are identical (Fig. 4), so the differences in the spectral characteristics should be attributed to those in their microstructures. Figure 2 shows that the film synthesized under CH_3NH_3I excess in the precursor solutions is more diffuse and the microcrystals display successive reduction in size along the (1 : 1)–(1 : 2)–(1 : 3) series, as also evident from a decrease in the integral absorption by the films (Fig. 5a). For denser films containing larger crystals the internal reabsorption of luminescence (the internal filter effect), which can lead to a red shift and to a decrease in its intensity, should also be more significant [29]. The film synthesized at a 1 : 1 ratio of components exhibits

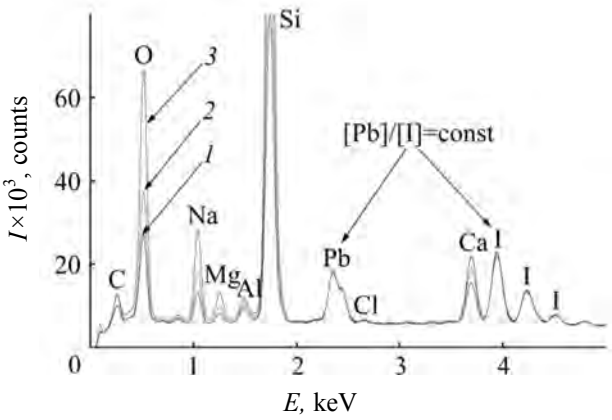

Fig. 4. EDX spectra of the $CH_3NH_3PbI_{2.98}Cl_{0.02}$ films heat-treated at 80°C and prepared at the PbI_2 : CH_3NH_3I ratio of (*1*) 1 : 1, (*2*) 1 : 2, and (*3*) 1 : 3. The spectrum exhibits peaks of the elements contained in the (Na_2O–MgO)–CaO–Al_2O_3–SiO_2 glass substrate [27].

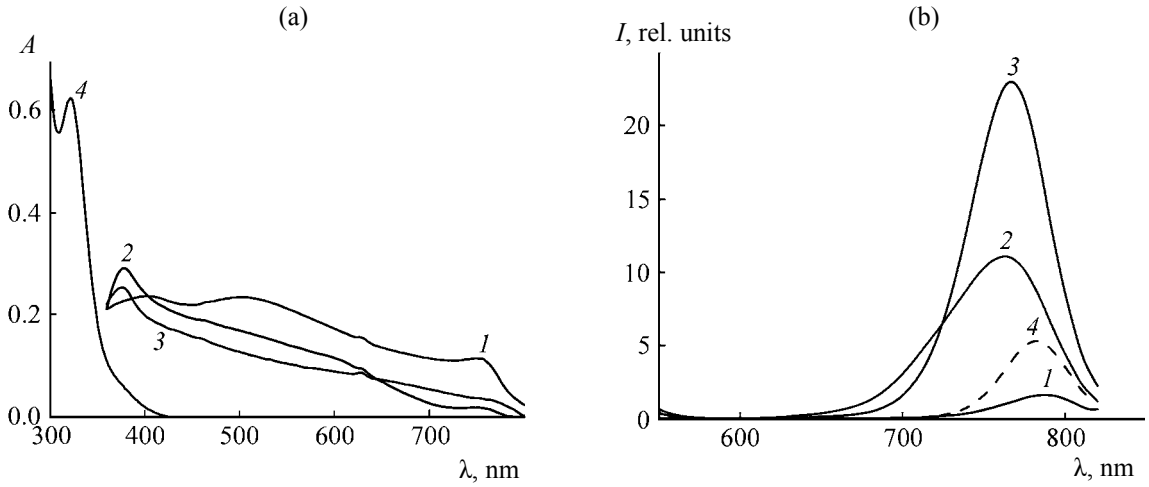

Fig. 5. (a) Normalized absorption spectra of (1–3) $CH_3NH_3PbI_{2.98}Cl_{0.02}$ films heat-treated at 80°C and prepared at the PbI_2 : CH_3NH_3I ratio of (*1*) 1 : 1, (*2*) 1 : 2, (*3*) 1 : 3, and of (*4*) precursor solution for the film deposition in DMF and (b) fluorescence spectra of the $CH_3NH_3PbI_{2.98}Cl_{0.02}$ films heat-treated at (*1–3*) 80 and (*4*) 150°C and prepared at the PbI_2 : CH_3NH_3I ratio of (*1*) 1 : 1, (*2*) 1 : 2, and (*3, 4*) 1 : 3; λ_{exc} = 450 nm.

a lower luminescence intensity compared to the films obtained at 1 : 2 and 1 : 3 ratios, although its optical density at the excitation wavelength (450 nm) is higher. The differences in the shapes of the fluorescence bands between the films synthesized at 1 : 2 and 1 : 3 ratios can be attributed to the same effect.

Thus, the synthesis of $CH_3NH_3PbI_3$ perovskite at a 1 : 1 ratio of the PbI_2 and CH_3NH_3I reactants both in air (55–65% humidity) and in a dry box (5–10% humidity) yielded a mixed-phase film. Partial substitution of the iodide by chloride ions led to a single-phase solid solution $CH_3NH_3PbI_{2.98}Cl_{0.02}$, in agreement with the published theoretical data on a stronger kinetic limitation for the $CH_3NH_3PbI_3 \rightarrow CH_3NH_3I + PbI_2$ degradation reaction in this system. A change in the reactant ratio alters the film morphology, and this is accompanied by an increase in absorption at 350–400 nm and by its decrease in the visible region of the spectrum, as well as by an increasing trend in the fluorescence intensity of the samples.

EXPERIMENTAL

As reactants we used lead iodide, methylammonium chloride (chemically pure), and presynthesized CH_3NH_3I [30]; dry dimethylformamide (chemically pure) served as solvent.

For preparation of $CH_3NH_3PbI_{3-x}Cl_x$ (x = 0, 0.02) films, the PbI_2, CH_3NH_3I, and CH_3NH_3Cl reactants in the required stoichiometric ratios were dissolved in DMF and stirred for 1 h at 70°C. Synthesis was carried out both in air (55–65% humidity) and in a dry box. The resulting solution was spin-coated on glass substrates at the substrate rotation speed of 20 or 40 rpm. The films were heat-treated for 30 min in a temperature range of 70–150°C. Synthesis of organic-inorganic perovskites $CH_3NH_3PbI_{3-x}Cl_x$ was carried out at different ratios of PbI_2 and CH_3NH_3I reactants (1 : 1, 1 : 2, 1 : 3).

The resulting films were identified by powder X-ray diffraction on a DRON-4-07 unit (CuK_α radiation). Microstructural examinations were performed using a MII-4 microinterferometer and a SEC mini-SEM SNE 4500MB scanning electron microscope. Elemental composition of the films was analyzed using an EDAX Element PV6500/00 F spectrometer coming with this microscope. Absorption and fluorescence spectra both of the perovskite films on glass substrates and of the precursor solutions in DMF were recorded on a Shimadzu-3100 spectrophotometer (Japan) and a Solar2203 spectrofluorimeter (Belarus), respectively.

REFERENCES

1. Mishra, A., Majumdar, B., and Ranjan, R., *J. Eur. Ceram. Soc*., 2017, vol. 37, no. 6, p. 2379. doi 10.1016/j.jeurceramsoc.2017.01.036
2. Jan, S.U., Zeb, A., and Milne, S.J., *J. Eur. Ceram. Soc*., 2017, vol. 36, no. 11, p. 2713. doi 10.1016/j.jeurceramsoc.2016.03.018.
3. V'yunov, O.I., Kovalenko, L.L., and Belous, A.G., *Inorg. Mater*., 2006, vol. 42, no. 12, p.1363. doi 10.1134/S0020168506120144

4. Plutenko, T.A., V'yunov, O.I., Belous, A.G., and Yanchevskii, O.Z., *J. Adv. Ceram*., 2016, vol. 5, no. 2, p. 117. doi 10.1007/s40145-016-0180-6
5. Belous, G. Novitskaya, G.N., Polyanetskaya, S.V., and Gornikov, Y.I., *Izv. Akad. Nauk SSSR, Neorg. Mater*., 1987, vol. 23, no. 3, p. 470.
6. Belous, A., Pashkova, E., Gavrilenko, O., V'yunov, O., and Kovalenko, L., *Ionics,* 2003, vol. 9, no. 1, p. 21. doi 10.1007/BF02376532
7. V'yunov, O.I., Belous, A.G., Tovstolytkin, A.I., and Yanchevskii, O.Z., *J. Eur. Ceram. Soc*., 2007, vol. 27, no. 13, p. 3919. doi 10.1016/j.jeurceramsoc.2007.02.063
8. Solopan, S.O., V'yunov, O.I., Belous, A.G., Polek, T.I., and Tovstolytkin, A.I., *Solid State Sci*., 2012, vol. 14, no. 4, p. 501. doi 10.1016/j.solidstatesciences.2012.01.030
9. Friedländer, S., Ovchar, O., Voigt, H. Böttcher, R., Belous, A., and Pöppl, A., *Appl. Magn. Reson*., 2015, vol. 46, no. 1, p. 33. doi 10.1007/s00723-014-0611-x
10. *Dielectric Material*, Silaghi, M.A., Ed., InTech, 2012, p. 113. doi 10.5772/51168
11. Belous, A.G., Yanchevskii, O.Z., V'yunov, O.I., Mazhara, N.V., and Kovalenko, L.L., *Inorg. Mater*., 2008, vol. 44, no. 4, p. 414. doi doi:10.1134/S002016850804016X
12. Ahn, C.W., Maurya, D., Park, C.S., Nahm, S., and Priya, S., *J. Appl. Phys*., 2009, vol. 105, no. 11, p. 114108. doi 10.1063/1.3142442
13. Im, J.-H., Lee, C.-R., Lee, J.-W., Park, S.-W., and Park, N.-G., *Nanoscale,* 2011, vol. 3, no. 10, p. 4088. doi 10.1039/C1NR10867K
14. Kim, H.-S., Lee, C.-R., Im, J.-H., Lee, K.-B., Moehl, T., Marchioro, A., Moon, S.-J., Humphry-Baker, R., Yum, J.-H., Moser, J.E., Grätzel, M., and Park, N.-G., *Sci. Rep*., 2012, vol. 2, p. 591. doi 10.1038/srep00591
15. Kim, H.-S., Im, S.-H., and Park, N.-G., *J. Phys. Chem. C*, 2014, vol. 118, no. 11, p. 5615. doi 10.1021/jp409025w
16. Kieslich, G., Sun, S., and Cheetham, A.K., *Chem. Sci*., 2014, vol. 5, no. 12, p. 4712. doi 10.1039/C4SC02211D
17. Leblebici, S.Y., Leppert, L., Li, Y., Reyes-Lillo, S.E., Wickenburg, S., Wong, E., Lee, J., Melli, M., Ziegler, D., Angell, D.K., Ogletree, D.F., Ashby, P.D., Toma, F.M., Neaton, J.B., Sharp, I.D., and Weber-Bargioni, A., *Nat. Energy*, 2016, vol. 1, p. 16093. doi 10.1038/nenergy.2016.93
18. Drisdell, W.S., Leppert, L., Sutter-Fella, C.M., Liang, Y., Li, Y., Ngo, Q.P., Wan, L.F., Gul, S., Kroll, T., Sokaras, D., Javey, A., Yano, J., Neaton, J.B., Toma, F.M., Prendergast, D., and Sharp, I.D., *ACS Energy Lett.*, 2017, vol. 2, no. 5, p. 1183. doi 10.1021/acsenergylett.7b00182
19. Wu, Y., Islam, A., Yang, X., Qin, C., Liu, J., Zhang, K., Penga, W., and Han, L., *Energy Environ. Sci.,* 2014, vol. 7, no. 9, p. 2934. doi 10.1039/C4EE01624F
20. Manser, J.S., Reid, B., and Kamat, P.V., *J. Phys. Chem. C*, 2015, vol. 119, no. 30, p. 17065. doi 10.1021/acs.jpcc.5b05898
21. Zhang, Y.-Y., Chen, S., Xu, P., Xiang, H., Gong, X.-G., Walsh, A., and Wei, S.-H., *arXiv. Condens. Matter*, 2015. arXiv:1506.01301 [cond-mat.mtrl-sci].
22. Jeon, N.J., Noh, J.H., Kim, Y.C., Yang, W.S., Ryu, S., and Seok, S.I., *Nat. Mater*., 2014, vol. 13, no. 9, p. 897. doi 10.1038/nmat4014
23. Kawamura, Y., Mashiyama, H., and Hasebe, K., *J. Phys. Soc. Jpn*., 2002, vol. 71, no. 7, p. 1694. doi 10.1143/JPSJ.71.1694
24. Baikie, T., Fang, Y., Kadro, J.M., Schreyer, M., Wei, F., Mhaisalkar, S.G., Graetzel, M., and White, T.J., *J. Mater. Chem. A*, 2013, vol. 1, no. 18, p. 5628. doi 10.1039/C3TA10518K
25. Cherezova, L.A., *Ionno-luchevye metody v opticheskoi tekhnologii* (Ion-Beam Methods in Optical Technology), St. Petersburg: Sankt-Peterb. Gos. Univ. Inf. Tekhol. Mekh. Opt., 2007, p. 126.
26. Horváth, O. and Mikó, I., *J. Photochem. Photobiol., A*, 1998, vol. 114, no. 2, p. 95. doi 10.1016/S1010-6030(98)00214-7
27. Barbieri, L., Ferrari, A.M., Lancellotti, I., Leonelli, C., Rincón, J.M., and Romero, M., *J. Am. Ceram. Soc.,* 2000, vol. 83, no. 10, p. 2515. doi 10.1111/j.1151-2916.2000.tb01584.x
28. González-Carrero, S., Galian, R.E., and Pérez-Prieto, J., *Part. Part. Syst. Charact*., 2015, vol. 32, no. 7, p. 709. doi 10.1002/ppsc. 201400214
29. Lakowicz, J.R., *Principles of Fluorescence Spectroscopy*, Berlin: Springer, 2011.
30. Qiu, J., Qiu, Y., Yan, K., Zhong, M., Mu, C., Yana, H., and Yang, S., *Nanoscale,* 2013, vol. 5, p. 3245. doi 10.1039/C3NR00218G